PHYSICAL REVIEW D VOLUME 11, NUMBER 7 1 APRIL 1975

Nucleon diffractive dissociation. I. Peripheral model with absorption

V. A. Tsarev*
Fermi National Accelerator Laboratory, Batavia, Illinois 60510†
(Received 26 August 1974)

A model for diffractive dissociation of hadrons into low-mass states is proposed. It is based on a peripheral mechanism with absorption. The absorption effects lead to an important modification of the amplitude by introducing an extra dependence upon momentum transfer and strong slope-mass correlation. A diffractive minimum is predicted for small values of the mass of the produced system. The connection with the crossover effects in diffractive dissociation is discussed. The nucleon dissociation is considered in detail.

I. INTRODUCTION

Diffractive dissociation of hadrons into low-mass multiparticle states has been studied for many years but still remains one of the most enigmatic phenomena in hadron physics. These processes, while inelastic, have most of the features of elastic scattering. This amazing similarity leads to the conclusion that the basic dynamics for elastic and diffractive dissociation reactions are the same. The general approach to understanding this phenomenon was outlined in the 1950's[1] and suggests that, as in optics, diffractive elastic and inelastic scattering is a result of absorption of different components of incoming waves. A hadron is considered as a set of virtual states which can be transformed into real particles by elastic scattering without the change of internal quantum numbers. A classic example is the regeneration of K_S from K_L through the different absorption of K and $\bar{K}$ in hadronic matter. Another example is the "vector-meson dominant" interaction of photons with hadrons.

Unfortunately, up to now there has been no explicit dynamical realization of this general idea which can explain in a completely satisfactory way all detailed features of diffractive dissociation. One of the most popular models is the double-peripheral model of the Drell-Hiida-Deck (DHD) type[2] which explains many important features of diffractive dissociation. However, recently some serious objections against this model were put forward which led to skepticism concerning its validity.

In this paper we show that the remedy for this model can be found by taking into account the absorption. This possibility of building upon and refining this model seems to us very important, especially since it is nearly the only model which gives explicit predictions for the dependence on all kinematical variables and involves a minimal number of free parameters.

In Sec. II the most important features of diffractive dissociation are discussed with emphasis on nucleon dissociation, which we chose as an explicit example in this paper.

Starting from the Good-Walker approach[1] we consider in Sec. III the derivation of the traditional DHD-type model for the processes $NN \to \pi NN$, $\pi\Delta N$, and σNN (where σ is an effective two-pion system). With some approximations we obtained a simple analytic expression for $d^2\sigma/dt\, dM_X^2$ which can be used in the missing-mass analysis.

Derivation of the DHD-type amplitude with absorption is done in Sec. IV. We show that the absorptive corrections introduce into the invariant matrix element an extra dependence on momentum transfer and slope-mass correlation.

These features were found necessary for agreement with experiment. The absorbed amplitude becomes more peripheral and a diffractive minimum arises for production of low-mass systems. The effect of the absorption on the crossover in diffractive dissociation is also discussed. In this paper we present only a qualitative discussion of the model. Detailed comparison with data will be given elsewhere.

II. LOW-MASS NONRESONANT ENHANCEMENTS IN DIFFRACTIVE DISSOCIATION

One of the most interesting problems in diffractive dissociation is connected with the properties of the produced system. Missing-mass distributions in diffractive dissociation of nucleons and π and K mesons exhibit strong enhancements in the low-mass region. Such peaks in mass spectra are usually interpreted as resonances. However, a detailed comparison with the phase-shift analysis shows that not all of these peaks have counterparts in the resonance spectrum found in formation experiments. Moreover, as has been shown recently by careful analysis of the dissociation

$\pi \to 3\pi$ [Ref. 3(a)] in the region of the A_1, A_2, and A_3 peaks, none of the partial waves except $J^P = 2^+$ (A_2) has resonance behavior, i.e., A_1 and A_3 enhancements *are not resonances*. Similar results have been found also for the $K\pi\pi$ system. [For a review see Ref. 3(b).] The other important fact is that most peaks produced in diffraction dissociation processes are not produced by any other reaction process (for example, in charge exchange). These facts mean that in addition to peaks corresponding to the excitation of "normal" resonances one should admit the existence of nonresonant enhancements.[4] Thus, we are faced with an extremely interesting question: What is the mechanism causing a "resonancelike" enhancement for the nonresonant amplitude at certain mass values? Here the experiment provides us with the very important information which, probably, is a key to the understanding of diffraction dissociation. It tells us that

(1) a hadron preferentially dissociates into two particles, one of which is always a pion ($X = X_1 + \pi$) (Ref. 5),

(2) the mass distribution usually peaks near the $M_{X_1} + \mu$ threshold;

(3) there is a reciprocal relationship between the slope of the differential cross section and the mass M_X of the produced system [typically the slope parameter is $\simeq 15$ (GeV/c)$^{-2}$ near threshold and decreases to 4–5 (GeV/c)$^{-2}$ at larger M_X], and

(4) in contrast to elastic scattering the diffractive system does not conserve s-channel helicity.

These properties, if understood, would lead to insight into the dynamics of diffractive dissociation.

The experimental data on mass spectra in nucleon excitation $N \to N^*$ are somewhat contradictory. All measurements agree that the most pronounced feature of the mass spectra at small t is a bump at $M_X \simeq 1.4$ GeV. But in some experiments this bump is found to be structureless,[6(a)] whereas in others[6(b)] some narrow peaks at $M_X \simeq 1.5$ and 1.7 GeV have been found. Similar structure has recently been found at high energies.[7(a)]

Sometimes there is a tendency to associate the bump at 1.4 GeV with the Roper resonance P_{11} found in the phase analysis of πN scattering at $M = 1470$ MeV. But this interpretation meets a number of difficulties:

(i) The contribution of the Roper resonance is much smaller than the contribution of $N^*(1500)$ and $N^*(1688)$ resonances and is not seen in the total πN cross section with $I = \frac{1}{2}$, but only in detailed partial-wave analysis. But in diffractive excitation the 1.4-GeV bump is a dominant feature at low mass and small t.

(ii) There is a significant shift of the peak position in production and formation experiments. In $N \to \pi N$ and $N \to \pi\pi N$ channels the peaks are observed at different masses (1250 and 1450 MeV) in contrast to the "normal" resonance decay (see, however, Ref. 8).

(iii) The width of the peak is much larger in production than in formation.

(iv) There is no reasonable explanation in the resonance model for a fast decrease of the slope parameter from 15–20 (GeV/c)$^{-2}$ at the $M_X \simeq M_N + \mu$ threshold to 5–7 at $M_X \sim 2$ GeV.

Another interpretation of the bump is connected with a DHD-type multiperipheral mechanism corresponding to the diagram shown in Fig. 1. This model successfully explains many characteristic features of diffractive dissociation, including the following:

(a) weak s dependence as a result of the approximate constancy of the πN scattering cross section at high energies,

(b) approximately equal cross sections for the dissociation of a particle and its antiparticle,

(c) approximate factorization,

(d) predominantly vacuum quantum number exchange, and

(e) preference for dissociation into an $X_1 + \pi$ system.

In this model some important features of diffractive dissociation arise from kinematics:

(i) The low-mass enhancement results from a phase-space factor which leads to the vanishing of the amplitude at the threshold and from a decreasing of the matrix element when going to larger M_X due to peripherality and kinematics.[9]

(ii) Strong M_X dependence of the slope parameter is a consequence of the double peripherality of Fig. 1: $T \propto \exp(Bt + B_1 t_1)$. At the threshold t and t_1 are linearly related and consequently $T \propto \exp[(B + B_1)t]$. As M_X becomes larger the dependence of t_1 on t becomes weaker, leading to weaker t dependence of T.

(iii) The difference in the peak positions for πN

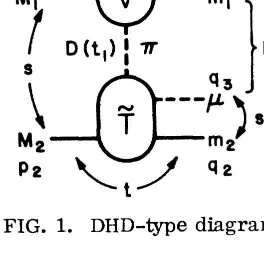

FIG. 1. DHD-type diagram.

and $\pi\pi N$ channels is naturally explained in terms of the different masses of the final states.

The DHD-type peripheral model in various modifications was successfully applied in analysis of π, K, and N diffractive dissociation in different regions of the kinematical variables. However, recently, some objections have been found against such interpretations of diffraction bumps.

Firstly, in a detailed analysis of the reaction $pp \to pn\pi^+$ as a function of all four variables it was pointed out[10] that pure kinematics is not sufficient to reproduce the whole M_X dependence of the slope parameter and that the data still show some extra M_X dependence of the slope which must be explicitly present in the invariant matrix element.

Secondly, for only one of the two crossovers observed in diffraction dissociation, $\pi^+ (\pi^-) \to A_1^+ (A_1^-)$, the DHD model gives the right prediction, whereas for the other, $K^0 (\bar{K}^0) \to Q^0 (\bar{Q}^0)$, it predicts a ratio of cross sections which is opposite to the data.[11] The fact that the relative normalizations of the K^0 and $\bar{K}^0$ differential cross sections are taken care of automatically through the natural composition of the K_L^0 makes this result very reliable.

These difficulties[12,13] are serious problems for the DHD-type model. We shall show that the possible way out is connected with absorption. The nucleon dissociation will be considered as an explicit example.

III. DOUBLE PERIPHERAL MODEL

We shall start from the Good-Walker model of diffractive dissociation.[1] According to this model, the incoming particle at large momentum in the target rest frame can be viewed as a fluctuating object with various fluctuations permitted by the quantum numbers:

$$|\lambda_{\text{in}}\rangle = \sum \alpha_{\text{in},k} |\tilde{\lambda}_k\rangle \ .$$

The components of the incoming wave $|\tilde{\lambda}_k\rangle$ interact with the target particle due to the elastic diffractive scattering caused by absorption, so that after scattering

$$|\lambda_{\text{fin}}\rangle = \sum \alpha_{\text{in},k}\, \eta_k |\tilde{\lambda}_k\rangle \ ,$$

where $|\eta_k| < 1$ are absorption parameters.

The scattered wave is the difference

$$\begin{aligned} |\lambda_{\text{sc}}\rangle &= |\lambda_{\text{in}}\rangle - |\lambda_{\text{fin}}\rangle \\ &= (1-\eta_{\text{in}})|\lambda_{\text{in}}\rangle + \sum_k (\eta_{\text{in}} - \eta_k)\alpha_{\text{in},k} |\tilde{\lambda}_k\rangle \ . \end{aligned} \tag{3.1}$$

The first term in Eq. (3.1) describes elastic scattering, whereas inelastic scattering (i.e., diffractive dissociation) is contained in the second one. One can see from Eq. (3.1) that the diffractive-dissociation amplitude is proportional to the difference between the amplitude for the absorption of the produced particles and the amplitude for the absorption of the incoming particle (Fig. 2).

The experimental evidence that the cross sections for diffractive production processes (σ_d) are about one order of magnitude smaller than that for the elastic one (σ_{el}) can be used[14] to show that to first order in ($\sigma_d/\sigma_{\text{el}}$) the scattering of a virtual component off the target can be approximated by the scattering of real particles.

We shall now apply this formalism to the case of nucleon dissociation $NN \to \pi NN$. Neglecting first double scattering in the final state, we have the diagrams shown in Fig. 3. Diagrams 3(a) and 3(b) have the same vertices but contain in general independent singularities in different channels $\bar{s}$ $(q_b + q_c)^2$ and $\bar{u} = (q_b - q_c)^2$. However, in the high-energy and small-momentum-transfer limit for the Reggeon, shown by the bubble in Fig. 3, $q^2 \simeq -q_\perp^2$. Then $q_0^2 = q_z^2$, so that

$$\bar{s} = m_a^2 + 2q_0(P_{a0} - P_{az}) + q^2 \ ,$$

$$\bar{u} = m_c^2 + 2q_0(P_{cz} - P_{c0}) + q^2$$

and, as $q^2 \to 0$, $\bar{s} \to m_a^2$ simultaneously $\bar{u} \to m_c^2$ and the contributions of diagrams 3(a) and 3(b) cancel each other (see also Ref. 9). It means that in the limit of high energies and small mass and momentum transfer the main contribution arises from diagram 3(c). Thus we come to the DHD model.[16]

At first sight it seems that it is very naive to expect that the amplitude Reggeon + $N \to \pi + N$ (entering the upper part of Fig. 1) can be adequately described at low M_X by only the pion pole. If one assumes similarity with the usual binary reactions then this approximation is definitely unreasonable at small $\bar{s}$. However, it is clear from the above discussion that neither in the physical picture of the reaction nor in the kinematics does one have full similarity for these reactions.

At very high momentum, it becomes reasonable to consider the incoming hadron as a superposition of "almost free" components and the high-energy kinematics stress the one important diagram. Experiment confirms the importance of this double peripheral diagram in diffractive dissociation.

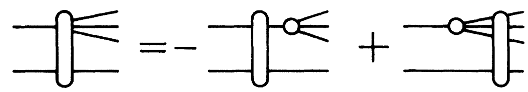

FIG. 2. Production amplitude in diffractive-dissociation model.

Now, let us calculate the contribution of Fig. 1. For further reference, we shall consider the general case when all particle masses are different. All necessary kinematical relations and definitions are given in the Appendix.

The cross section for reaction $NN \to \pi NN$ is

$$d\sigma = (2\pi)^{-5} s^{-1} (m_1 m_2 M_1 M_2) \sum |T_0|^2 \frac{d^3q_1\, d^3q_2\, d^3q_3}{q_{10} q_{20} q_{30}} . \tag{3.2}$$

Choosing as independent variables the invariants $s, t, \bar{s} = M_X{}^2$, and angles θ and ϕ between $\vec{p}_1$ and $\vec{q}_1$ in the system where $\vec{q}_1 + \vec{q}_3 = 0$, we can rewrite Eq. (3.2) as

$$\frac{d\sigma}{d\bar{s}\, dt\, d\phi\, d\cos\theta} = (2\pi)^{-4} \frac{m_1 m_2 M_1 M_2}{2s^2} \frac{q}{M_X} |T_0|^2 . \tag{3.3}$$

The matrix element for Fig. 1 can be written in the following form:

$$T_0 = G_r V(t_1) D(t_1) \tilde{M}_{\pi N}(s_1, t, t_1) F(t, t_1) . \tag{3.4}$$

Here G_r is a rationalized and renormalized πNN-coupling constant $G_r{}^2/4\pi = 14.4$. V is a spin part of the vertex, and

$$\sum_{\text{spin}} |V|^2 = -\frac{t_1}{4m_1 M_1} . \tag{3.5}$$

The meson propagator $D(t_1)$ can be chosen either in the elementary particle form

$$D_{\text{el}}(t_1) = (\mu^2 - t_1)^{-1} \tag{3.6}$$

or in the Reggeized form[17]

$$D_R{}^2(t_1) = \frac{(\pi\alpha_\pi')^2}{2(1 - \cos\pi\alpha_\pi)} (\xi/\xi_0)^{2\alpha_\pi} , \tag{3.7}$$

where the π trajectory is $\alpha_\pi = \alpha_\pi'(t_1 - \mu^2)$. In Eq. (3.7)

$$\xi = \bar{s} - t - M_1{}^2 + (m_1{}^2 - M_1{}^2 - t_1)(\mu^2 - t_1 - t)/2t_1$$

and ξ_0 is a scale factor.

We shall use the following approximation for Eq. (3.7):

$$D_R{}^2(t_1) \simeq D_{\text{el}}{}^2(t_1) \exp\left[2\alpha_\pi' \ln\left(\frac{M_X{}^2 - M_1{}^2}{\xi_0}\right) (t_1 - \mu^2)\right] .$$

We assume that the off-shell πN scattering amplitude $\tilde{M}_{\pi N}$ can be approximated by the on-shell amplitude $M_{\pi N}$, so that at large s and small t

$$\tfrac{1}{2} \sum |\tilde{M}_{\pi N}|^2 = \frac{e^{b_{\pi N} t}}{m_2 M_2} [\sigma_t^{\pi N}(s_1) q_3^P(s_1)^{1/2}]^2 , \tag{3.8}$$

where we neglect the small contribution of the real part of the πN scattering amplitude. (q_3^P is the momentum in the system where $\vec{q}_2 + \vec{q}_3 = 0$.) Comparison with experimental data [see, for example, Ref. 7(a)] indicates that the amplitude must have some additional t_1 and t dependence, which we choose here in the simplest form

$$F(t, t_1) = F_1(t_1) F_2(t) ,$$

with

$$F_i(x) = \exp[\delta_i (x - \mu^2)] .$$

Such extra t_1 and t dependence turns out to be quite sizeable and is usually attributed to the off-shell effects. In Sec. IV, we shall give another interpretation of this dependence.

Using Eqs. (3.4)–(3.8) we can write Eq. (3.3) as

$$\frac{d\sigma}{dt\, d\bar{s}\, d\phi\, d\cos\theta} = R_1(-t_1)(t_1 - m^2)^{-2} \times [q_3^P(s_1)^{1/2}]^2 \exp[\delta(t_1 - \mu^2)] , \tag{3.9}$$

where

$$R_1 = \frac{1}{8\pi^2} \left(\frac{\sigma_{\pi N}}{4\pi}\right)^2 \left(\frac{G_r}{s}\right)^2 \exp[(b_{\pi N} + \delta_2) t] \frac{q}{M_X}$$

and

$$\delta = \delta_1 \quad \text{for elementary } \pi ,$$

$$\delta = \delta_1 + 2\alpha_\pi' \ln\left(\frac{M_X{}^2 - M_1{}^2}{\xi_0}\right) \quad \text{for Reggeized } \pi .$$

At large energies we shall neglect the weak s_1 dependence of $\sigma_{\pi N}$. Then only $[(q_3^P)^2 s_1]$ in Eq. (3.9) depends upon ϕ. Integration over ϕ leads to the following form useful in the analysis of t, M_X, and t_1 ($\equiv a + b\cos\theta$) distributions:

$$\frac{d\sigma}{dt\, d\bar{s}\, d\cos\theta} = R_1 R_2 (-t_1)(t_1 - \mu^2)^{-2} \times \exp[\delta(t_1 - \mu^2)] .$$

where

$$R_2 = \tfrac{1}{2}\pi (A_+ + B\cos\theta)(A_- + B\cos\theta) + \tfrac{1}{2} C^2 \sin^2\theta . \tag{3.10}$$

Further integration over θ gives the missing-mass cross section:

$$\frac{d^2\sigma}{dt\, d\bar{s}} = \frac{\pi R_1}{4qp_1} [\Phi(x_-) - \Phi(x_+)] , \tag{3.11}$$

where

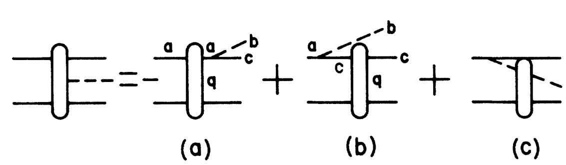

FIG. 3. Diagrams for $NN \to \pi NN$ dissociation.

$$\Phi(x) = e^{\delta x}\left(\frac{\gamma}{\delta}x - \frac{\gamma}{\delta^2} + \frac{\beta+\mu^2\gamma}{\delta} - \frac{\mu^2\alpha}{x}\right) + \mathrm{Ei}(\delta x)(\alpha+\mu^2\beta+\mu^2\alpha\delta),$$

$\mathrm{Ei}(x)$ is the exponential integral function, $x_\pm = a - \mu^2 \pm b$, and the kinematical variables a, b, α, β, and γ are defined in the Appendix.

The M_X and t dependence of the cross section (3.11) has the gross features found in experiment: the bump in M_X near threshold $(M_N+\mu)$ and the rise of the slope parameter when M_X approaches threshold.[18] The extra t_1 dependence due to $F_1(t_1)$ leads to suppression of the cross section especially at larger M_X and to a shift of the maximum in the M_X distribution to smaller M_X (see Fig. 4). The Reggeization has a similar effect with even stronger suppression of larger M_X.

As an example, we show in Fig. 5 the comparison of Eq. (3.11) with recent data on $pp\to Xp$ and $pd\to Xd$ diffractive dissociation.[7] [More details can be found in Ref. 7(b)].

If we suggest that the whole experimental peak near $M_X \simeq 1.4$ GeV is connected with $p\to p+\pi^0$ and $p\to n+\pi^+$ dissociation then we need $\delta_1 \approx 2$ $(\mathrm{GeV}/c)^{-2}$ and $\delta_2 \approx 3$ $(\mathrm{GeV}/c)^{-2}$ to have a reasonable absolute value and the peak position. Even with these large values of δ_1 and δ_2 the value of the slope is still smaller than in the experiment. If we accept that there are other contributions in this M_X region, we need even stronger suppression of the absolute value. In Sec. IV we show that the t and t_1 dependence and suppression in the absolute value can be obtained from absorption.

As far as the other contributions are concerned, we assume that at low M_X they are connected with

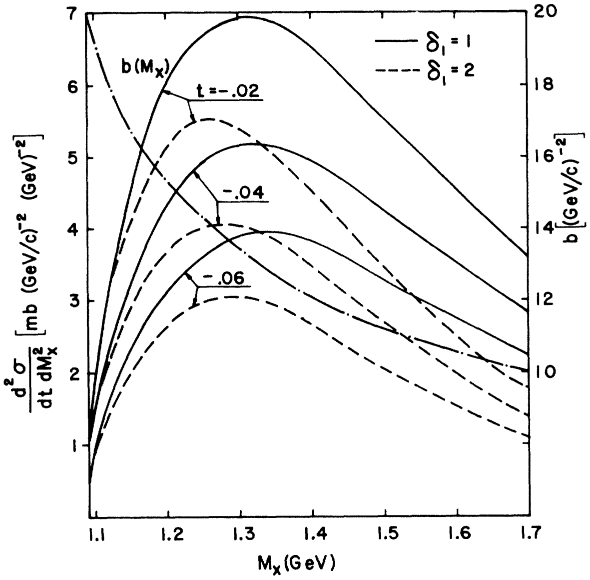

FIG. 4. Mass distribution and slope parameter from Eq. (3.11) for non-Reggeized pion with $\delta_1 = 1$ and 2, $\delta_2 = 3$ $(\mathrm{GeV}/c)^{-2}$, $\sigma_{\pi N} = 24$ mb, and $b_{\pi N} = (9\ \mathrm{GeV}/c)^{-2}$.

two-pion production $(N\to\pi\pi N)$. For small values of M_X the two-pion–nucleon channel can be described in this model through the channels $N\to\pi\Delta$ and $N\to\sigma N$, where Δ is a 33 isobar and σ is a "scalar meson" which effectively takes into account the enhancement in the two-pion system near threshold [diagrams (a) and (b) in Fig. 6].

The corresponding contributions can be easily obtained from (3.4), noting the difference in couplings and in ths spin structure of πNN and $\Delta N\pi$, σNN vertices. This leads to the substitution in

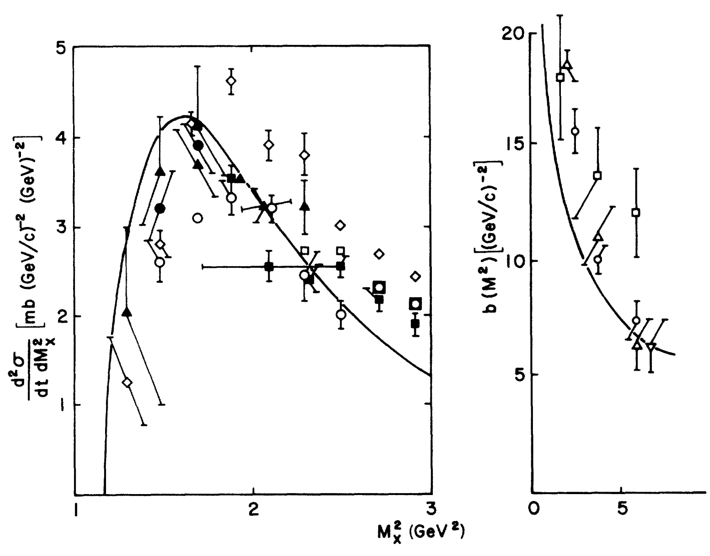

FIG. 5. Comparison of Eq. (3.11) with data from Ref. 7.

(3.10) and (3.11):

$$\sigma_{\pi N}{}^2\left(\frac{G_{\pi NN}{}^2}{4\pi}\right) \to \begin{cases} \dfrac{\sigma_{\pi N}{}^2}{\pi^2}\displaystyle\int_\Delta q M_X{}^2 \sigma_{\pi N}(M_X{}^2)\, dM_X & (\text{“}\Delta\text{”}) \\ \dfrac{G_{\sigma NN}{}^2}{4\pi}\sigma_{\sigma N}{}^2 (M_1+m_1)^2\,, & (\text{“}\sigma\text{”}) \end{cases}$$

$$\Phi(x) \to \Phi_1(x) = e^{\delta x}\left(\frac{\gamma}{\delta} - \frac{\alpha}{x}\right) + \mathrm{Ei}(\delta x)(\beta + \alpha\delta)\,. \tag{3.12}$$

The effective coupling for the "Δ case" can be calculated from the πN cross section (or the Δ isobar width). For the "σ case" neither $G_{\sigma NN}$ nor $\sigma_{\sigma N}$ is known experimentally.

Both diagrams have nearly the same threshold and lead to similar M_X and t dependence, shown in Fig. 7. The characteristic feature of both diagrams connected with scalar coupling is the larger value of the slope near the corresponding threshold than for the diagram with $N \to \pi N$ dissociation.

It is reasonable to assume that the missing-mass peak at $M_X \sim 1.4$ GeV is a superposition of those diagrams corresponding to $N \to \pi N$ and $N \to \pi\pi N$ dissociation.

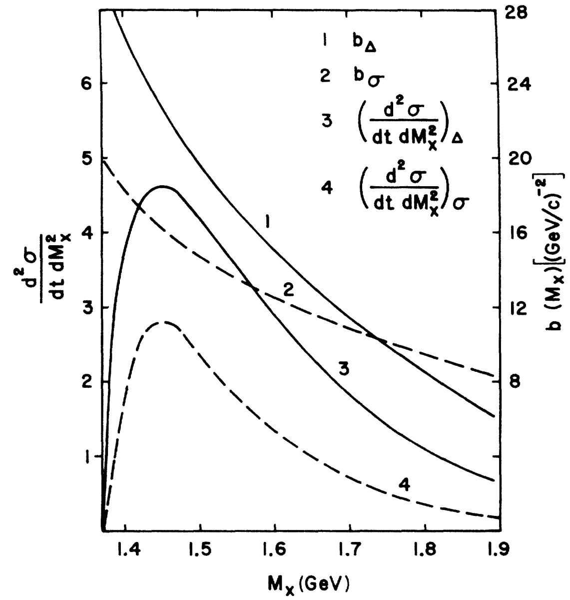

FIG. 7. Mass distribution at $t = -0.02$ $(\mathrm{GeV}/c)^2$ (arbitrary normalization) and slope parameter for Fig. 6.

IV. ABSORPTION

In Sec. III we considered the process (Fig. 1) where an incoming nucleon interacts with the target by means of emission of a pion which in turn scatters diffractively on a target. Simultaneously with this "indirect" interaction, the nucleon must also interact "directly" with the target (waved lines in Fig. 8). It is well known that such absorption effects, connected with distortion of incoming and scattered waves, play an important role in binary reactions, leading to the substantial modification of the "unabsorbed" amplitudes. In this section we present a model for absorptive corrections to diffractive dissociation.

We shall suggest that similarly to the binary reaction case (see, for example Ref. 19), absorption can be taken into account using the S matrix of elastic scattering of particles in the initial (S_i) and final (S_f) states:

$$T(\vec{\rho}_j) = S_i{}^{1/2}(\vec{\rho}_j)\, T_0(\vec{\rho}_j) S_f{}^{1/2}(\vec{\rho}_j)\,. \tag{4.1}$$

Here $T_0(\vec{\rho}_j)$ is the unabsorbed amplitude of Sec. III in the impact-parameter representation[20]

$$T_0(\vec{\rho}_j) = (2\pi)^{-3}\int \prod_{j=1}^{3} d^2k_j\, e^{i\vec{k}_j\cdot\vec{\rho}_j}\, T(\vec{k}_j)\, \delta^2\Big(\sum_{j=1}^{3}\vec{k}_j\Big)\,. \tag{4.2}$$

$\vec{k}_j$ is the two-dimensional transverse (with respect to $\vec{p}_1$) component of momentum $\vec{q}_j$ and $\vec{\rho}_j$ is the two-dimensional impact parameter conjugate to the $\vec{k}_j$. [We work here in the over-all center-of-mass system $(\vec{p}_1 + \vec{p}_2 = 0)$.]

The absorbed amplitude $T(\vec{k}_j)$ can be found from Eq. (4.1) with the inverse transformation

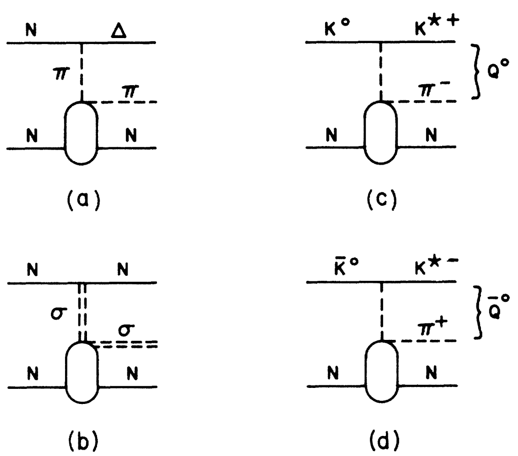

FIG. 6. DHD-type diagrams for dissociation $NN \to \pi\Delta N$, $NN \to \sigma NN$, and $K^0(\bar{K}^0) \to Q^0(\bar{Q}^0)$.

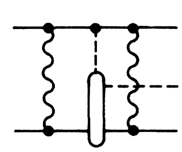

FIG. 8. Double peripheral amplitude with the absorption.

$$T(\vec{k}_j) = 9(2\pi)^{-1}\int \prod_{j=1}^{3} d^2\rho_j\, e^{-i\vec{k}_j\cdot\vec{\rho}_j}\, T(\vec{\rho}_j)\,\delta^2\Big(\sum_{j=1}^{3}\vec{\rho}_j\Big)\,. \tag{4.3}$$

In general, S_f describes rescattering of all particles in the final state. In particular, for M_X near a resonance, the resonance interaction between the produced particles may be important. Here, however, we are interested in a nonresonant mechanism giving rise to a bump. Therefore, we shall restrict our consideration here to the region near threshold $M_1+\mu$ where the resonance interaction presumably can be neglected. Since in the first approximation (i.e., in T_0) we have already taken into account the direct pion-target interaction, we are left with the nucleon-target interaction in the final state. In other words, we can consider the produced system as a quasiparticle which interacts with target as a nucleon so that

$$S_i = S_f = S_{\rm el}\,,$$

where

$$S_{\rm el} = 1 + \frac{1}{4\pi}\, T_{\rm el} \tag{4.4}$$

is the S matrix of elastic nucleon-nucleon scattering. However, the presence of the pion in the final state still affects absorption. The reason is that the absorption depends upon the helicities of the particles. The relative motion of the produced particles generates "spin" of the quasiparticle. The higher M_X, the more orbital states of the produced system with different helicities are important.

Let T_0^n be an amplitude (corresponding to Fig. 1) which describes the production of particles 1 and 3 with helicity n along $\vec{p}_i$.[21] We can define it as

$$T_0^n(\vec{k}) = \frac{1}{2\pi}\int_0^{2\pi} e^{-in\psi}\, T_0(\psi,\vec{k})\,, \tag{4.5}$$

where ψ is the angle between the planes $\vec{q}_1, \vec{q}_3$ and $\vec{q}_2, \vec{p}_1$ (Fig. 9).

It is clear that in our approximation only one impact parameter is relevant which we choose to be conjugate to $\vec{k}$, the transverse component of $\vec{q}_2$,

$$\vec{k}^2 = \vec{q}_2^{\,2}\sin^2\theta_2^c \simeq -t\,. \tag{4.6}$$

Then instead of Eq. (4.2) and (4.3) we can use

$$T^n(k) = \int_0^\infty \rho\, d\rho\, T_0^n(\rho)\, S_{\rm el}(\rho)\, J_n(\rho k) \tag{4.7}$$

and

$$T_0^n(\rho) = \int_0^\infty k\, dk\, T_0^n(k)\, J_n(\rho k)\,, \tag{4.8}$$

where $J_n(x)$ is the Bessel function.

In the diffractive peak region the elastic nucleon-nucleon scattering amplitude can be parametrized as

$$T_{\rm el}(s,t) = (i+\alpha)\sigma e^{bt/2}\,, \tag{4.9}$$

where σ is the total NN cross section and b is the slope parameter. α is the ratio of the real to the imaginary parts of the elastic NN scattering amplitude. At high energies it is experimentally small and will be neglected.[22] From Eqs. (4.8) and (4.9)

$$S_{\rm el}(\rho) = 1 - (\sigma/4\pi b)\, e^{-\rho^2/2b}\,. \tag{4.10}$$

Thus absorption leads, just as in the binary case, to suppression of low impact parameters.

Substituting (4.8) into (4.9) and using form (4.10) for $S_{\rm el}(\rho)$ one obtains

$$T^n(k) = T_0^n(k) - \delta T^n(k)\,,$$

where

$$\delta T^n(k) = \frac{\sigma}{4\pi}\exp(\tfrac{1}{2}tb) \times \int_0^\infty k'\, dk'\, T_0^n(k')\exp(-\tfrac{1}{2}k'^2 b)\, I_n(k'kb) \tag{4.11}$$

and $I_n(x)$ is a Bessel function of complex argument. A similar equation for the binary reaction case was obtained by Henyey *et al.*[23] Using the expression for T_0 from Sec. III and kinematical formulas given in the Appendix one can perform the integration in Eq. (4.11). These calculations and the detailed comparison with experiment will be given elsewhere. Here we restrict ourselves to qualitative discussion.

First we note that, if the final-state scattering is known, the absorption will involve no free parameters (as is the case for reaction $NN\to\pi NN$). Unfortunately, in diffractive dissociation the final-state particles X_1 are usually unstable (ρ, K^*, Δ, etc.) whose elastic scattering is unknown.[24] Thus a simplifying assumption must be made (for example, that the final-state scattering is the same as the initial one). The other source of uncertain-

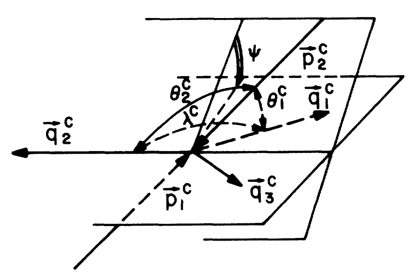

FIG. 9. Kinematics in the center-of-mass system.

ty is connected with inelastic absorption. From experience with binary reactions it is known that the real absorption is stronger than follows from the elastic prescription. This fact is usually attributed to the contribution of diffractive inelastic scattering which effectively enlarges the rescattering cross section. These effects are usually taken into account phenomenologically[25] by the change

$$\sigma_{\mathrm{el}} \to \lambda\sigma_{\mathrm{el}} \quad (\lambda > 1)\,.$$

The other effect of inelastic rescattering could be to change the effective slope $b \to \xi b$.

To make our qualitative discussion more transparent, we shall start from a simple model for the amplitude T_0. We choose instead of $(\mu^2 - t_1)^{-1}$ an exponential form for the upper peripheral part of Fig. 1 so that

$$T_0 \simeq A e^{(Bt + B_1 t_1)/2}\,, \tag{4.12}$$

and we neglect the t and t_1 dependence of A.

The integration over ψ in Eq. (4.5) involves only t_1. Noting that

$$t_1 = r_1 + r_2 \cos\psi\,, \tag{4.13}$$

where

$$\begin{aligned} r_1 &= m_1{}^2 + M_1{}^2 - 2q_{10}^c p_{10}^c \\ &\quad + 2q_1^c p_1^c \cos\theta_2^c \cos\lambda^c\,, \\ r_2 &= 2q_1^c p_1^c \sin\theta_2^c \sin\lambda^c\,, \end{aligned} \tag{4.13$'$}$$

one gets from (4.5) and (4.12)

$$T_0^n = A e^{(Bt + B_1 r_1)/2} I_n(\tfrac{1}{2} B_1 r_2)\,. \tag{4.14}$$

In both limits $t \to 0$ ($\theta_2^c \to \pi$) and $M_X \to m_1 + \mu$ ($\lambda^c \to \pi$) the argument in (4.14) vanishes and

$$I_n(\tfrac{1}{2} B_1 r_2) \to \frac{(\frac{1}{4} B_1 r_2)^n}{\Gamma(n+1)}\,. \tag{4.15}$$

Let us first consider production of the system with M_X near the threshold. One can then see immediately from Eq. (4.15) that only the nonflip amplitude ($n = 0$) is important. In this limit from Eq. (4.13′) $r_1 \simeq t$ and

$$T_0 \simeq T_0^0 \simeq A e^{(B + B_1)t/2}\,. \tag{4.16}$$

Substituting (4.16) into (4.11) we obtain the following expression for the absorbed amplitude (M_X near the threshold):

$$T(t) = T_0(t)\phi(t)\,,$$

where

$$\phi(t) = \left[1 - \frac{\sigma}{4\pi(B + B_1 + b)} \exp\left(-\frac{t}{2}\,\frac{(B + B_1)^2}{B + B_1 + b}\right)\right] \tag{4.17}$$

If we fix M_X not too close to threshold, then for some limited range of t we can also fix t_1. Then $T(t, t_1) = T_0(t, t_1)\phi(t_1, t_2)$ and

$$\phi(t, t_1) = \left[1 - \frac{\sigma}{4\pi(B + B_1 + b)} \exp\left(-\frac{t_1 B_1}{2} - \frac{t}{2}\,\frac{B^2 + BB_1 - bB_1}{B + B_1 + b}\right)\right]\,. \tag{4.17$'$}$$

These expressions display the following important features of diffractive dissociation:

(i) From Eqs. (4.14) and (4.15) we have a simple explanation for the experimental fact that for production of low-mass states near the threshold the s-channel helicity is approximately conserved but for larger M_X it is not.

(ii) Absorption introduces extra t (and t_1) dependence into the amplitude, leading to a very steep differential cross section near threshold (Fig. 10). This dependence, as discussed in Sec. IV, is found necessary from a comparison with experiment and is usually attributed to the off-shell effects. In contrast to the factorized t and t_1 dependence due to the form factors, Eq. (4.17) leads to coupled t and t_1 dependence. This can be used for experimental distinguishing of these forms.

(iii) At some $t = t^*$ expression (4.17) vanishes, leading to a minimum in the low-mass diffractive-dissociation cross section. A rough estimation based on Eq. (4.17) with $B \simeq B_1 \simeq b \simeq 10$ (GeV/c)$^{-2}$ and $\sigma \sim 40$ mb gives for t^* the value $\simeq 0.2$ (GeV/c)^2 (Fig. 10). The contributions from $n \neq 0$ states fill in this minimum. These contributions become more important at larger M_X, leading to disappearance of the dip. A similar conclusion about a minimum at small M_X was obtained recently in Ref. 26 from a different approach. Experiment[27] seems to confirm this prediction.

(iv) One can also speculate that the factor $\phi(t)$ · may explain the crossover in $K^0(\overline{K}^0) \to Q^0(\overline{Q}^0)$ diffractive dissociation (Fig. 6). At present it is difficult to say anything more definitive since the cross sections and slopes for $K^{*\pm}$-N scattering are unknown as well as the effect of inelastic absorption. In order for the factor ϕ to act in the right direction we need to assume that the relation between the $\sigma(K^{*+}N)$ and $\sigma(K^{*-}N)$ cross sections is different from that between $\sigma(K^+N)$ and $\sigma(K^-N)$. The possibility for verification of the model can be obtained from the measurements of the crossover in the reactions

$$pp \to \pi^+ np(\pi^0 pp),$$
$$\bar{p}p \to \pi^- \bar{n}p(\pi^0 \bar{p}p).$$

If inelastic absorption is negligible ($\lambda = \xi = 1$) the absorptive corrections can be expressed in terms of the known values of the cross sections and slopes for pp and $\bar{p}p$ scattering.

Now, let us consider production of the system with large M_X. We shall see that the dramatic strengthening of the t dependence of the amplitude due to absorption found near the threshold disappears as M_X increases.

At large M_X one can neglect the t dependence of r_2 and, using (4.15), integrate (4.17). Then

$$\delta T^n = \frac{\sigma}{4\pi(B+b)} e^{-tB^2/2(B+b)} T_0^n \left(\frac{b}{B+b}\right)^n . \quad (4.18)$$

We see from (4.18) that the relative magnitude of the absorptive corrections $\delta T^n/T_0^n$ decreases with increasing n due to the factor $[b/(B+b)]^n$. It means that the contributions of higher n become more important in the absorbed amplitude than in the unabsorbed. However, we know from (4.15) that at small t, T^n behaves as $(\sqrt{-t})^n$. Thus the change in the relative contribution of different helicity states caused by absorption leads to the flattening of the t dependence at large M_X.

The importance of absorption and spin effects for diffractive dissociation was already emphasized by Kane *et al.*[28] and the properties (i), (ii), (iii), and (v) were discussed from a general assumption of peripherality of diffractive processes. Recently on this basis a phenomenological model was constructed[26] where the peripheral shape and strength of different n-states were chosen *ad hoc*. In our approach we have an explicit dynamical mechanism for both.

Summing up T^n [inverse to (4.5)] and using (4.18) we obtain (for $t_1 \simeq 0$) the full amplitude of the form $T = T_0 \tilde{\phi}$, where

$$\tilde{\phi} = 1 - \frac{\sigma}{4\pi(B+b)} \exp\left[t\, \frac{B(B_1 - B)}{2(B+b)} \right] . \quad (4.19)$$

Typically $B \simeq B_1$ and $\tilde{\phi}$ is practically independent of t. Thus, comparing with (4.17), we obtain another important property of the model:

(v) Absorption makes the slope of the amplitude increase as M_X approaches the threshold.

It is clear that the properties found for the amplitude with exponential t_1 dependence will also hold for the original form

$$T_0 = Ae^{Bt/2}(\mu^2 - t_1)^{-1} .$$

In this case instead of (4.14) we obtain

$$T_0^n = Ae^{Bt/2} Q_n(t) , \quad (4.14')$$

where

$$Q_n(t) = \frac{1}{(\bar{r}_1^{\,2} - r_2^{\,2})^{1/2}} \left(\frac{\bar{r}_1 - (\bar{r}_1^{\,2} - r_2^{\,2})^{1/2}}{r_2} \right)^n$$

and $\bar{r}_1 = \mu^2 - r_1$.

At $t \to 0$ or $M_X \to m_1 + \mu$

$$Q_n(t) \simeq \frac{1}{\bar{r}_1} \left(\frac{r_2}{2\bar{r}_1} \right)^n . \quad (4.15')$$

$\bar{r}_1, r_2$ are functions of t:

$$\bar{r}_1 = l_1 + l_2 t, \quad r_2 = a\sqrt{-t} ,$$

where

$$\left.\begin{aligned} l_1 &= \mu^2 + 2q_{10}^c p_{10}^c - m_1^{\,2} - M_1^{\,2} \\ &\quad + (2q_{20}^c p_{20}^c - m_2^{\,2} - M_2^{\,2}) \cos\lambda^c , \\ l_2 &= \frac{q_1^c}{q_2^c} \cos\lambda^c , \end{aligned}\right\} \quad (4.20)$$

$$a = \frac{2p_1^c q_1^c}{q_2^c} \sin\lambda^c . \quad (4.21)$$

Now we can integrate (4.11) using the approximate form (4.15′), and the small-t limit for $I_n(k'kb) \simeq (k'kb/2)^n/n!$.

The resulting expression for the amplitude T^n is

$$T^n(t) = T_0^n \left[1 - \frac{\sigma}{8\pi} \exp\left(\frac{b-B}{2}\, t \right) P_n(t) \right], \quad (4.22)$$

where

$$P_n(t) = (n!)^{-2} (\tfrac{1}{2} b)^n (\tilde{r}_1)^{n+1} \frac{d^n}{dl_2^{\,n}} \left(\frac{e^{-Z}}{l_2} \mathrm{Ei}(Z) \right)$$

and

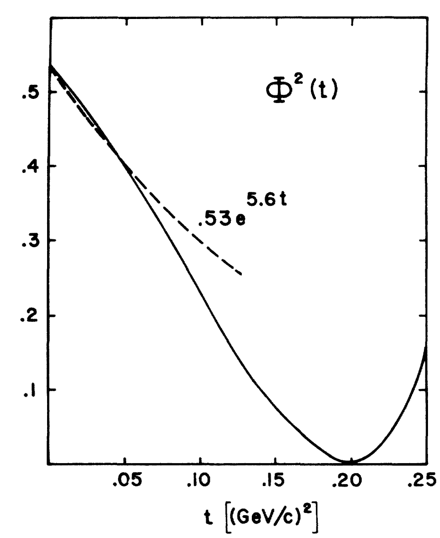

FIG. 10. Absorptive factor $\Phi^2(t)$. For comparison at small t the function 0.53 exp(5.6t) is shown.

$$Z \equiv l_1(B+b)/2l_2 .$$

The cross section can be calculated now as in Sec. III with $|T_0|^2 \to \sum_n |T^n|^2$.

ACKNOWLEDGMENTS

I would like to thank G. Fox, E. Jenkins, S. Mukhin, and A. R. White for useful discussions and G. Takhtamyshev for help in numerical calculations.

APPENDIX

We list here some kinematical variables for Fig. 1.

Metric:

$$p^2 = p_0^2 - \vec{p}^2 .$$

Invariants:

$$s = w^2 = (p_1+p_2)^2, \quad t = (q_2 - p_2)^2 ,$$

$$\bar{s} = M_X^2 = (q_1+q_2)^2 , \quad t_1 = (q_1 - p_1)^2 ,$$

$$s_1 = (q_2 + q_3)^2, \quad \bar{t} = (q_2 - p_1)^2 .$$

Symbols:

$$E(x, y, z) = (2x)^{-1}(x + y - z) ,$$

$$P(x, y, z) = (2x)^{-1}[x^2 - 2x(y+z) + (y-z)^2]^{1/2} .$$

In the rest system of the fragments ($\vec{q}_1 + \vec{q}_3 = 0$) one has

$$p_{10} = E(M_X^2, M_1^2, t) ,$$

$$q_{30} = E(M_X^2, \mu^2, m_1^2) ,$$

$$q_{10} = E(M_X^2, m_1^2, \mu^2) ,$$

$$p_{20} = E(M_X^2, M_2^2, \bar{t}) ,$$

$$p_1 = P(M_X^2, M_1^2, t) ,$$

$$q_1 = q_3 = P(M_X^2, m_1^2, \mu^2) ,$$

$$p_2 = P(M_X^2, M_2^2, \bar{t}) ,$$

and

$$\bar{t} = m_2^2 + M_1^2 + M_2^2 - M_X^2 - s - t .$$

Angles:

Between $\vec{q}_1$ and $\vec{p}_1$,

$$\cos\theta = \frac{1}{2qp_1}(2q_{10}p_{10} - m_1^2 - M_1^2 + t_1) ;$$

between $\vec{p}_1$ and $\vec{p}_2$,

$$\cos\alpha = \frac{1}{2p_1p_2}(2p_{10}p_{20} + M_1^2 + M_2^2 - s) ;$$

between $\vec{q}_1$ and $\vec{p}_2$,

$$\cos\epsilon = \cos\alpha \cos\theta + \sin\alpha \sin\theta \cos\phi .$$

One can express the invariants s_1 and t_1 in the system where $\vec{q}_1 + \vec{q}_3 = 0$:

$$s_1 = A + B\cos\theta + C \sin\theta \cos\phi ,$$

where

$$A = s + m_1^2 - 2q_{10}(p_{10} + p_{20}) ,$$

$$B = 2q(p_1 + p_2 \cos\alpha) ,$$

$$C = 2qp_2 \sin\alpha ,$$

$$t_1 = a + b\cos\theta ,$$

$$a = m_1^2 + M_1^2 - 2q_{10}p_{10} ,$$

$$b = 2qp_1 ,$$

and

$$(q_3^P)^2 s_1 = 4^{-1}[(A_+ + B\cos\theta)(A_- + B\cos\sigma) + C\sin\phi(A_+ + A_- + 2B\cos\theta) + C^2\sin^2\theta\cos^2\phi] ,$$

$$A_\pm = A - (m_2 \pm \mu)^2 .$$

In our discussion of absorption we use the overall center-of-mass system ($\vec{p}_1 + \vec{p}_2 = 0$). Here

$$p_{10}^c = E(s, M_1^2, M_2^2), \quad p_{20}^c = E(s, M_2^2, M_1^2) ,$$

$$p_1^c = p_2^c = k^c = P(s, M_1^2, M_2^2) ,$$

$$q_{10}^c = E(s, m_1^2, s_1), \quad q_1^c = P(s, m_1^2, s_1) ,$$

$$q_{20}^c = E(s, m_2^2, M_X^2), \quad q_2^c = P(s, m_2^2, M_X^2) .$$

Angles:

Between $\vec{p}_1^c$ and $\vec{q}_1^c$,

$$\cos\theta_1^c = -\frac{1}{2k^c q_1^c}(-t_1 + m_1^2 + M_1^2 - 2p_{10}^c q_{10}^c);$$

between $\vec{p}_1$ and $\vec{q}_2$,

$$\cos\theta_2^c = \frac{1}{2k^c q_2^c}(-t + m_2^2 + M_2^2 - 2p_{20}^c q_{20}^c) ;$$

between $\vec{q}_1$ and $\vec{q}_2$,

$$\cos\lambda^c = \frac{1}{2q_1^c q_2^c}(-s + M_X^2 + s_1 - \mu^2 + 2q_{10}^c q_{20}^c) .$$

$$\alpha = A_+A_- + \frac{C^2}{2}\left(1 - \frac{d^2}{b^2}\right) + B\frac{2d^2}{b^2} - \frac{d}{b}B(A_+ + A_-) ,$$

$$\beta = \frac{B}{b}(A_+ + A_-) - \frac{2d}{b^2}\left(B^2 - \frac{C^2}{2}\right) ,$$

$$\gamma = \frac{B^2 - \frac{1}{2}C^2}{b^2} ,$$

where

$$d = a - \mu^2 .$$

*Permanent addresses: Joint Institute for Nuclear Research, Dubna, and P. N. Lebedev Physical Institue, Moscow, USSR.

†Operated by Universities Research Association Inc. under contract with the United States Atomic Energy Commission.

[1]An excellent summary has been prepared by E. L. Feinberg and I. Ia. Pomeranchuk, Nuovo Cimento Suppl. 3, 652 (1956); see also M. L. Good and W. D. Walker, Phys. Rev. 120, 1854 (1960).

[2]S. D. Drell and K. Hiida, Phys. Rev. Lett. 7, 199 (1961); R. Deck, *ibid.* 13, 1969 (1964).

[3](a) G. Ascoli, Phys. Rev. Lett. 25, 962 (1970); 26, 929 (1971); Phys. Rev. D 7, 669 (1973). (b) K. Lanius, report at the Fifth International Symposium on Many Particle Hadrodynamics, Leipzig, 1974 (unpublished).

[4]D. R. O. Morrison, rapporteur's talk, in *High Energy Physics*, proceedings of the Fifth International Conference on High Energy Physics, Kiev, 1970, edited by V. Shelest (Naukova Dumka, Kiev, U.S.S.R., 1972).

[5]H. J. Lubatti, Acta Phys. Pol. B 3, 721 (1972).

[6](a) K. Boesebeck *et al.*, Nucl. Phys. B28, 368 (1971); M. L. Longo *et al.*, Phys. Lett. 36B, 560 (1971); E. Colton *et al.*, Phys. Rev. D 3, 1063 (1971); M. Graessler *et al.*, Nucl. Phys. B 47, 43 (1972); P. Kobe *et al.*, *ibid.* B52, 109 (1973); Y. Gnat *et al.*, *ibid.* B54, 333 (1973); D. Hochman *et al.*, *ibid.* B80, 45 (1974); B80, 189 (1974). (b) E. W. Anderson *et al.*, Phys. Rev. Lett. 16, 855 (1966); R. M. Edelstein *et al.*, Phys. Rev. D 5, 1073 (1972); J. V. Allaby *et al.*, Nucl. Phys. B 52, 316 (1973).

[7](a) B. Bartenev *et al.*, Phys. Lett. B 51, 299 (1974); Y. Akimov *et al.*, Fermilab Reports Nos. NAL-Conf-74/56 Exp and NAL-Conf-74/66 Exp, 1974 (unpublished). (b) Y. Akimov *et al.*, Fermilab Report No. FERMILAB-Conf-74/79-THY/EXP, 1974 (unpublished).

[8]F. Von Hippel and C. Quigg, Phys. Rev. D 5, 624 (1972).

[9]L. Stodolsky, Phys. Rev. Lett. 18, 973 (1967).

[10]H. I. Miettinen and P. Pirilä, Phys. Lett. 40B, 127 (1972).

[11]R. E. Diebold, in *Proceedings of the XVI International Conference on High Energy Physics, Chicago-Batavia, Ill., 1972,* edited by J. D. Jackson and A. Roberts (NAL, Batavia, Ill., 1973), Vol. 3, p. 1.

[12]Another experimental fact which is usually considered as evidence against DHD-type models is a small cross section for interaction of the produced system in nuclei (see Ref. 13). However, in the multiperipheral model particles are created over an extended region of space-time. Some of them miss the target. This leads to a decrease of the nuclear scattering, and the DHD-type model can be reconciled with experiment.

[13]A. S. Goldhaber *et al.*, Phys. Rev. Lett. 22, 802 (1969); W. Beusch, Acta Phys. Pol. B3, 679 (1972).

[14]A. Białas, W. Czyż, and A. Kotanski, Ann. Phys. (N.Y.) 73, 439 (1972).

[15]V. N. Gribov, in *Proceedings of XVI International Conference on High Energy Physics, Chicago-Batavia, Ill., 1972,* edited by J. D. Jackson and A. Roberts (Ref. 11), Vol. 3, p. 491.

[16]We want to stress that the arguments about cancellations work only in the case $t_1 \simeq 0$. The missing-mass kinematics obeys this condition at small t only with the additional assumption $\bar{s} \simeq s_{\text{thresh}}$. As $\bar{s}$ rises, the kinematically allowed region for t_1 extends and contributions of Figs. 3(a) and 3(b) may become important.

[17]E. Berger, Phys. Rev. 166, 1525 (1968).

[18]It is interesting to note that at large enough M_X values the slope parameter becomes smaller than $(b_{\pi N} + \delta_2)$, i.e., there is a "partial compensation" of peripherality due to extending of the phase space.

[19]For a review see J. D. Jackson, Rev. Mod. Phys. 37, 494 (1965).

[20]F. S. Henyey, Phys. Lett. 45B, 364 (1973).

[21]We are interested here in an effect of relative motion of produced particles, and we ignore for simplicity the nucleon spin or equivalently assume nucleon helicity conservation: $(\lambda_1 - \lambda_2) - (\lambda_1' - \lambda_2') = 0$. Then n is a net s-channel helicity flip.

[22]V. Bartenev *et al.*, Phys. Rev. Lett. 31, 1367 (1973). For the sake of simplicity we leave out many details in the present consideration, which can be taken into account in more exact calculations. For example, it is clear now that the Pomeron is not a simple pole, at least at the present energies, but here we make this approximation; we neglect also its shrinkage and so on.

[23]F. Henyey *et al.*, Phys. Rev. 182, 1579 (1969).

[24]In principle, the cross section and slope parameter for scattering of unstable particles can be found from experiments on nuclei.

[25]M. Ross, F. Henyey, and G. L. Kane, Nucl. Phys. B23, 269 (1970).

[26]S. Humble, Nucl. Phys. B76, 137 (1974).

[27]CERN-Hamburg-Orsay-Vienna Collaboration (E. Nagy *et al.*), submitted to the XVII International Conference on High Energy Physics, London, 1974 (unpublished).

[28]G. Cohen-Tannoudji, G. L. Kane, and C. Quigg, Nucl. Phys. B37, 77 (1972); G. L. Kane, Acta Phys. Pol. B3, 845 (1972).